A Risk-Based Geospatial Optimization Framework for UAV Maritime Surveillance Path Planning in the North Natuna Sea

Adi, A. P.,* Aritonang, S., Sarjito, A. and Navalino R. D. A.
Defense Science, Republic of Indonesia Defense University, Indonesia
E-mail: anang8088@gmail.com,* ORCID ID: 0000-0002-9289-240X
**Corresponding Author*

DOI: https://doi.org/10.52939/ijg.v22i3.4877

Abstract
Maritime surveillance in strategically critical waters remains challenged by severe operational constraints limited fuel allocation, restricted vessel availability, and constrained aircraft endurance, creating extensive surveillance gaps in designated Areas of Responsibility (AoR). This research develops a risk-based geospatial optimization framework for Unmanned Aerial Vehicle (UAV) maritime surveillance path planning that explicitly addresses these surveillance gaps. The framework integrates four methodological stages: (1) strategic context analysis using PESTLE-SWOT and Analytical Network Process for optimal platform selection, (2) geospatial risk surface modeling using Kernel Density Estimation (KDE) applied to 159 historical maritime violations spanning 2021–2023, (3) multi-objective path optimization balancing threat detection efficiency with operational constraints, and (4) quantitative validation through comparative analysis with baseline routes. KDE analysis reveals highly non-uniform threat distribution across the study area, with significant violation clustering in specific geographic hotspots. Critically, the AoR encompasses extensive Low Risk Zones (83.3% of total area) that represent unmonitored regions where illicit activities possess higher potential to occur undetected due to sparse conventional patrol coverage. These Low-Risk Zones are not inherently safe but rather surveillance gaps requiring persistent monitoring. The optimized UAV route strategically allocates surveillance resources to cover both High-Risk concentration zones and the critical Low Risk areas, achieving 89.3% risk coverage efficiency and 43.7% improvement in threat detection efficiency compared to conventional uniform-coverage baseline routes. The optimized route spans 2,447 km, completed within 13.59 hours of flight time, well within UAV endurance constraints. This research provides a scientifically rigorous framework that integrates geospatial risk modeling with multi-objective optimization, moving beyond conventional geometric path planning toward a data-driven, threat-aware surveillance strategy. The methodology demonstrates that systematic identification and coverage of surveillance gaps particularly in Low-Risk Zones significantly enhances Maritime Domain Awareness and maritime security effectiveness.

Keywords: Geospatial Risk Modeling, Kernel Density Estimation, Maritime Surveillance, North Natuna Sea, Unmanned Aerial Vehicle (UAV)

1. Introduction

Indonesia, as the world's largest archipelagic state, faces immense challenges in ensuring maritime security, particularly in the North Natuna Sea [1]. This region is not only a vital economic corridor but also a geopolitical hotspot characterized by overlapping sovereignty claims and frequent "grey zone" operations [2]. Data from the Indonesian Navy confirms the strategic urgency, with over 159 recorded sovereignty violations between 2020 and 2023, including numerous encounters with foreign coast guard and naval vessels [3]. The North Natuna Sea contains valuable fisheries resources and energy reserves, which has triggered tensions with neighboring states. China, for instance, has consistently claimed large portions of the South China Sea, including Indonesia's Exclusive Economic Zone (EEZ) in the Natuna area, through its "Nine Dash Line" concept, which was rejected under the 1982 UNCLOS [4]. Repeated incursions by foreign fishing vessels (FFVs), escorted by the China Coast Guard (CCG), reflect China's grey zone operations defined as the use of non-military coercion to pressure the sovereignty of another state without triggering open armed conflict [5] and [6].

These provocative acts not only disrupt regional stability but also test Indonesia's credibility in safeguarding its maritime sovereignty. This situation reinforces Mahan's (1890) classic view that command of the sea constitutes a fundamental element in ensuring a nation's survival and prosperity [7]. Efforts by the Indonesian Navy to secure the North Natuna Sea through the deployment of warships (KRI) and maritime patrol aircraft (MPA) face significant limitations. Fuel allocation only permits two KRIs to operate alternately, while CN-235 and NC-212 MPA flights are restricted to 2–3 hours per day [8] and [3]. Such an operational pattern is far from ideal to cover the entire Area of Responsibility (AoR), which spans tens of thousands of square kilometers. Consequently, the effectiveness of conventional patrols remains low, reducing the ability to conduct comprehensive maritime surveillance [9].

To address these constraints, the use of Unmanned Aerial Vehicles (UAVs) emerges as a strategic alternative. UAVs offer several advantages, including low operational cost, long endurance, and flexibility in reaching areas inaccessible to KRIs or manned aircraft [10] and [11]. Moreover, modern UAVs are equipped with electro-optical sensors, high-resolution cameras, and real-time communication systems, enabling effective Intelligence, Surveillance, and Reconnaissance (ISR) operations [12]. With such capabilities, UAVs can significantly enhance Indonesia's Maritime Domain Awareness (MDA), which is essential for detecting, identifying, and responding to maritime threats [13] [14] and [15]. The use of technologies like the Automatic Identification System (AIS) has become a cornerstone of MDA, providing critical vessel tracking capabilities [16]. Several countries have already integrated UAVs into their naval defense systems, considering crucial aspects like human factors in their operational deployment [17]. The United States has developed the Large Unmanned Surface Vessel (LUSV), Israel deploys the Elbit Hermes UAV, and Norway utilizes the Hugin Endurance for maritime patrol missions [18]. Indonesia, therefore, must adapt quickly to this technological trend to strengthen its deterrence effect in the North Natuna Sea. Failure to modernize maritime patrol strategies risks the loss of control over strategic waters, as highlighted by defense analysts [19] and [20].

The next challenge, however, lies in designing UAV patrol routes that are both efficient and effective. In practice, UAV route planning must account for technical parameters such as patrol area coordinates, sensor field of view (FoV), flight altitude, speed, and endurance. Without proper route planning, UAV patrols risk being suboptimal in terms of coverage and energy consumption. This aligns with [21], who argue that mathematical models and algorithm-based planning are essential to balance area coverage and operational efficiency. A significant body of existing literature on UAV path planning, often termed Coverage Path Planning (CPP), has been surveyed extensively [22]. This research has predominantly focused on simplistic geometric patterns like lawnmower or spiral trajectories [23]. While computationally simple, these methods are fundamentally flawed for complex surveillance missions because they operate on the naive assumption that the operational area is a homogenous, risk-neutral space. This approach is inefficient, as it allocates surveillance assets equally to both high-threat and low-threat zones.

Recent advancements in geoinformatics and operations research have highlighted the need for more intelligent, risk-aware planning frameworks. As noted by [23], the integration of geospatial data is critical for creating accurate maritime risk analytics. Similarly, the concept of multi-objective optimization, balancing conflicting goals such as maximizing threat detection and minimizing operational cost, has become a central theme in modern vehicle routing problems, including maritime search and rescue and resource allocation for MDA [24] and [25]. Yet, a significant research gap persists in the development of a holistic framework that integrates strategic operational context, geospatial risk modeling, and multi-objective path optimization specifically for maritime surveillance. This study directly addresses this gap. We propose and validate a novel risk-based geospatial optimization framework for UAV maritime surveillance. Our contribution is threefold: (1) we introduce a methodology to construct a geospatial risk surface map from historical threat data, transforming the surveillance area into an intelligent, data-driven battlespace; (2) we formalize the UAV path planning problem as a multi-objective optimization task, moving beyond simple geometric coverage; and (3) we implement and test a heuristic algorithm that generates risk-adaptive routes, demonstrating a quantifiable improvement over conventional methods. By doing so, this research offers a significant methodological advancement in the field of geoinformatics, providing a scientifically robust and operationally superior decision-support tool for real-world maritime security operations.

2. Methodology

This research employs an integrated four-stage methodological framework that combines strategic analysis, multi-criteria decision-making, geospatial

risk modeling, and heuristic optimization to develop an intelligent UAV maritime surveillance system in North Natuna Sea (see Figure 1). The framework is designed to address the research gap identified in the introduction by moving beyond conventional geometric path planning toward a scientifically rigorous, data-driven approach that accounts for the non-uniform spatial distribution of maritime threats. Each stage of the framework builds sequentially upon the previous one, creating a coherent progression from strategic justification through technical implementation and validation. The overall approach integrates both qualitative and quantitative data collection methods, following a sequential exploratory mixed-method design that ensures both strategic relevance and technical rigor.

2.1 PESTLE-SWOT Strategic Analysis

PESTLE-SWOT analysis was conducted to evaluate the internal and external factors influencing maritime surveillance operations in the North Natuna Sea. The PESTLE framework examines six external dimensions Political, Economic, Social, Technological, Legal, and Environmental while the SWOT analysis identifies internal Strengths and Weaknesses, as well as external Opportunities and Threats. The PESTLE-SWOT analysis was conducted through a mixed-method approach combining qualitative and quantitative data collection. In the qualitative phase, semi-structured interviews were conducted with 10 subject matter experts (SMEs) from defense, maritime security, and technology sectors to identify key strategic factors and operational constraints. These interviews, lasting 45-60 minutes each, focused on understanding the current state of maritime surveillance, existing challenges, and potential benefits of autonomous vehicle deployment. Following the qualitative exploration, a structured questionnaire was distributed to 50 respondents with relevant expertise in maritime security, defense technology, and operational planning. Respondents were asked to rate the importance and impact of each PESTLE-SWOT factor using a 5-point Likert scale (1 = Not Important, 5 = Very Important). The scoring methodology employed for the PESTLE-SWOT analysis calculated both weights and ratings for each identified factor. The weight (W) represents the relative importance of the factor, calculated as the sum of all respondent ratings divided by the product of the number of respondents and the maximum scale value. The rating (R) reflects the perceived level of impact or severity of the factor on a 1-5 scale. The score for each factor was then calculated as the product of weight and rating ($S = W \times R$).

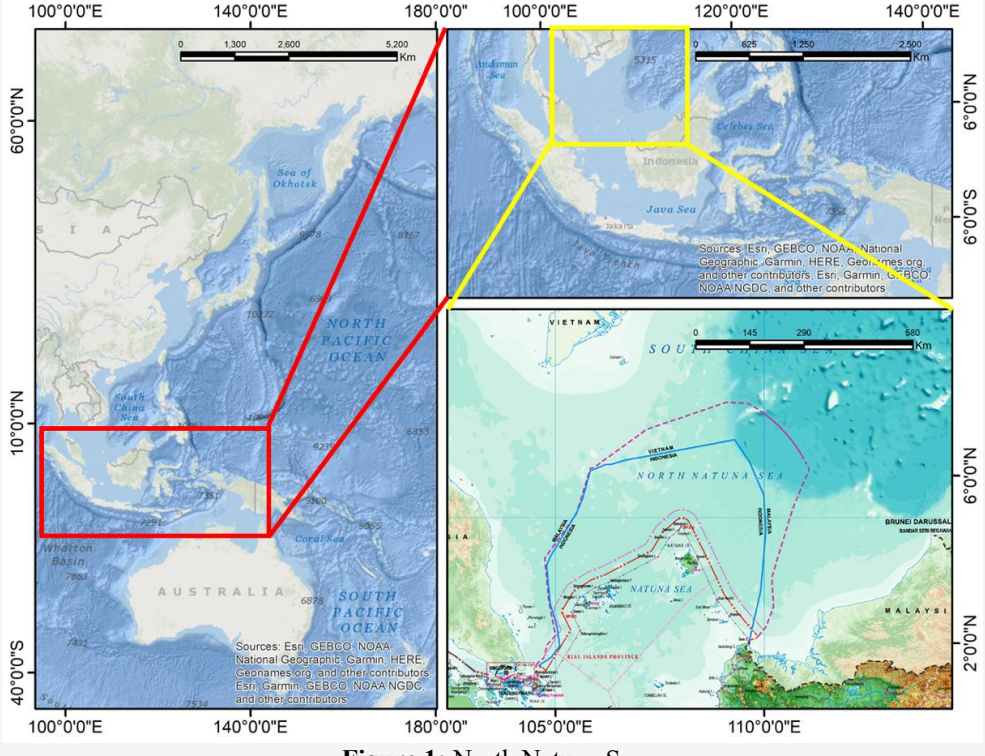

Figure 1: North Natuna Sea

The Internal Factor Analysis Summary (IFAS) was computed by summing the scores for all Strengths and Weaknesses, while the External Factor Analysis Summary (EFAS) was computed by summing the scores for all Opportunities and Threats. These summary scores were then plotted on a two-dimensional matrix to determine the strategic positioning of the organization and identify the most appropriate strategic response.

The results of the PESTLE-SWOT analysis indicated an Internal Factor Analysis Summary (IFAS) score of 0.043445 and an External Factor Analysis Summary (EFAS) score of -0.011064. These values positioned the strategic response in Quadrant II of the SWOT matrix, indicating a "Diversification Strategy" posture one that leverages internal strengths to mitigate external threats. This strategic context underscores that a technologically advanced, cost-effective, and efficient surveillance solution is not merely beneficial but essential for maintaining maritime security in the North Natuna Sea. The analysis confirmed that autonomous vehicle technology, when properly optimized, can address key operational weaknesses (such as high operational costs and limited coordination between agencies) while capitalizing on existing strengths (government support, technological readiness, and strategic location).

2.2 Analytical Network Process (ANP) for Optimal Platform Selection

The research employed the Analytical Network Process (ANP), a sophisticated multi-criteria decision-making (MCDM) method that explicitly accounts for feedback and interdependencies among evaluation criteria. The ANP framework was structured as a hierarchical network with four distinct levels. The goal level specified the objective of selecting the optimal autonomous vehicle platform for maritime surveillance in the North Natuna Sea. The criteria level consisted of four major evaluation dimensions: Capability (encompassing technical performance and operational capability), Cost (addressing financial considerations including acquisition, operational, and maintenance costs), Operational (evaluating operational feasibility and integration with existing systems), and Maintenance (assessing maintainability and support requirements). The sub-criteria level included fourteen specific sub-criteria distributed across the four criteria: under Capability were Endurance, Range, Cruise Speed, and Payload Capacity; under Cost were Acquisition Cost, Operational Cost, and Maintenance Cost; under Operational were Data Security, Sensor System, Communication System, and Navigation System; and under Maintenance were Spare Parts Availability, Human Resources, and Facilities. The alternatives level consisted of four autonomous vehicle platforms: UAV (Unmanned Aerial Vehicle), USV (Unmanned Surface Vehicle), AUV (Autonomous Underwater Vehicle), and UCAV (Unmanned Combat Aerial Vehicle).

Expert judgment was collected from 10 subject matter experts with deep knowledge of autonomous vehicle systems and maritime operations. These experts were asked to perform pairwise comparisons at each level of the hierarchy using the Saaty scale (1-9), where 1 represents equal importance, 3 represents weak importance, 5 represents strong importance, 7 represents very strong importance, and 9 represents absolute importance. The ANP analysis yielded clear and decisive results at the Alternatives Level. The UAV emerged as the optimal platform with a priority weight of 0.509, substantially higher than the second-ranked AUV (0.281), followed by UCAV (0.136) and USV (0.074). All consistency ratios were well below the 0.10 threshold (CR = 0.031), indicating highly reliable and consistent expert judgments. The UAV's superiority stems from multiple factors. At the sub-criteria level, UAV achieved the highest priority weights in critical performance dimensions: Endurance (0.513), Range (0.526), Cruise Speed (0.523), and Sensor System (0.530). These capabilities enable wide-area surveillance with minimal downtime and extended operational range.

Additionally, UAV demonstrated favorable performance in cost considerations, with an Acquisition Cost priority of 0.482 and Operational Cost priority of 0.461, indicating that while not the cheapest platform, it offers the best balance of capability and cost. The UAV also scored highly on operational criteria, with Data Security priority of 0.529 and Communication System priority of 0.514, ensuring reliable integration with existing command and control systems. Finally, the UAV exhibited favorable maintenance profiles with Spare Parts priority of 0.498 and SDM (human resources) priority of 0.517, reflecting the maturity and widespread adoption of UAV technology globally. This rigorous, data-driven selection process provides a scientifically defensible foundation for the subsequent optimization stages, ensuring that the path planning algorithm is applied to the most suitable platform for the operational context.

2.3 Area of Responsibility (AoR) Definition and Mathematical Modeling

2.3.1 Study area and AoR definition

The Area of Responsibility (AoR) is defined as the designated maritime region assigned to Koarmada I Tanjung Pinang for regular patrol operations and

maritime security enforcement. The study area selected for this research is designated as Sector X-3 within the North Natuna Sea (see Figure 2), which is characterized by significant geopolitical sensitivity due to its proximity to disputed maritime boundaries and the Nine Dash Line claim by China. Sector X-3 is bounded by six coordinate points: Point D (06°18′12″N – 109°38′33″E), Point E (05°31′00″N – 109°49′00″E), Point F (04°42′00″N – 109°52′00″E), Point H (04°42′00″N – 110°27′00″E), Point I (06°11′06″N – 111°03′17″E), and Point J (06°57′25″N – 110°33′35″E). These six points form a closed polygon encompassing the operational area. The selection of this specific sector is justified by its strategy.

2.3.2 AoR area calculation using shoelace formula

The total area of the AoR polygon was calculated using the Shoelace Formula (also known as the Surveyor's Formula), a mathematical method for computing the area of a polygon given its vertex coordinates. The Shoelace is defined in Equation 1:

$$A = \frac{1}{2}\left|\sum_{i=1}^{n} x_i y_{i+1} - x_{i+1} y_i\right| \quad \text{Equation 1}$$

Where x_i, and y_i are the coordinates of the polygon vertices, and n is the total number of vertices. The formula was implemented in MATLAB to calculate the area of Sector X-3. The calculation yielded a total AoR area of 25.391,09 km², which represents the total maritime zone requiring surveillance coverage. This large operational area underscores the need for efficient path planning to maximize coverage within the constraints of UAV endurance and operational time.

2.3.3 UAV flight path design and waypoint generation

Two conventional flight path patterns were designed to provide baseline comparisons for the optimized path. The first pattern, designated as the North-South (N-S) route, consists of parallel flight lines oriented in the north-south direction, creating a lawnmower pattern that systematically covers the entire AoR. The second pattern, designated as the East-West (E-W) route, follows the same lawnmower principle but with flight lines oriented in the east-west direction. For both routes, waypoints were generated at regular intervals to guide the UAV along the planned path. The waypoint spacing was determined based on the sensor swath width and the desired overlap percentage to ensure complete coverage of the operational area. A total of 100 waypoints were distributed along each baseline route, spaced at approximately 2.5 km intervals.

2.3.4 Sensor swath width calculation

The sensor swath width, representing the ground area covered by the UAV's camera sensor during a single pass, is a critical parameter for path planning.

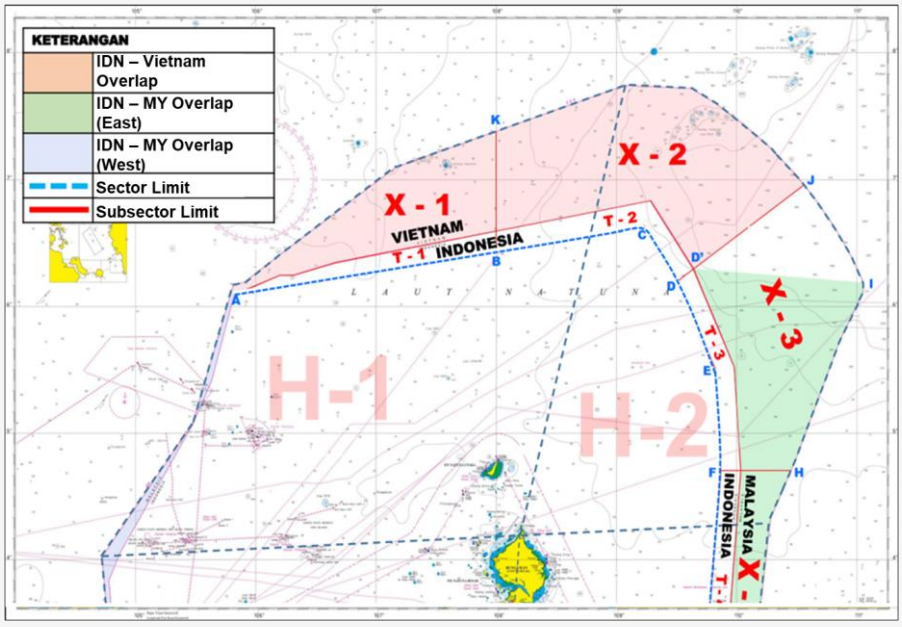

Figure 2: Patrol Area of Koarmada I in the North Natuna Sea

The swath width is calculated based on the UAV's altitude and the camera's field of view (FoV) using Equation 2:

$$W = 2h \cdot \tan\left(\frac{FOV}{2}\right)$$

Equation 2

Where W = swath width, h = UAV height from the ground (meters), FoV = Field of View angle (rad.). For this research, the following parameters were specified: Altitude (h): 1,828 meters (6,000 feet), Field of View (FoV): 150 degrees, Calculated Swath Width: Approximately 6,850 meters (6.85 km) The swath width calculation ensures that the UAV's sensor can effectively cover a substantial ground area with each pass, enabling efficient surveillance of the large AoR. The altitude of 1,828 meters was selected as a compromise between sensor resolution (which improves at lower altitudes) and operational safety (which improves at higher altitudes away from ground-based threats).

2.3.5 Waypoint spacing and overlap calculation

To ensure complete coverage of the AoR without gaps, waypoints are spaced with a specified overlap percentage. The spacing between parallel flight lines (d) is calculated using Equation 3:

$$d = W\left(1 - Overlap\right)$$

Equation 3

Where: d is the spacing between flight lines (meters), W is the swath width (meters), *Overlap* is the desired overlap percentage (typically 0.25). For the baseline routes, an overlap of 25% was specified, resulting in a spacing of approximately 5,138 meters (5.14 km) between parallel flight lines. This overlap ensures that adjacent sensor swaths overlap slightly, preventing coverage gaps that could allow violations to go undetected. The 25% overlap percentage is a standard practice in aerial surveillance missions, balancing the need for complete coverage with operational efficiency. The waypoint density was set at 100 waypoints per route, distributed along the flight path at regular intervals of approximately 2.5 km.

2.3.6 UAV flight parameters

The baseline routes were designed using the following UAV specifications and operational parameters in Table 1. These parameters were selected to approximate the operational conditions of UAVs employed by the Indonesian Navy and align with the requirements of modern maritime operations [9] and [10]. The combination of speed, endurance, and sensor FoV enables UAVs to conduct large-scale patrols with wide area coverage. Adjusting these parameters is essential to ensure that the simulation outcomes can be realistically implemented in actual maritime patrol operations.

2.4 Geospatial Risk Surface Modeling

2.4.1 Historical violation data and geocoding

Building upon the AoR definition and baseline path design, the research incorporates geospatial risk analysis to move beyond uniform coverage toward intelligent, threat-aware surveillance. The foundation of the geospatial risk surface is historical data on sovereignty violations in the North Natuna Sea. A comprehensive dataset was compiled spanning the period 2020-2023, comprising 159 recorded sovereignty violations. The data were collected from multiple authoritative sources including Indonesian Navy operational records, Bakamla (Indonesian Coast Guard) reports, and open-source maritime intelligence databases. The dataset includes various incident types such as unauthorized vessel entry, illegal fishing activities, resource exploitation, and naval confrontations. The spatial coverage encompasses the entire North Natuna Sea region, with particular focus on the study area (Sector X-3) covering 25,391 km².

Table 1: Parameters for developing the UAV AoR algorithm model

Parameter	Value	Description
Altitude	1,828 meter (6,000 feet)	The altitude at which the UAV flies toward Area X-3 LNU.
Field of View (FoV)	150°	The viewing angle covered by the UAV's camera sensor.
Overlapping	25% (0.25)	The portion of the image that overlaps with the previous image.
Cruise Speed	180 km/hour	The UAV's flight speed.
Endurance	30 hour	The maximum duration the UAV can remain airborne.

Each incident was geocoded to its precise latitude and longitude coordinates using the WGS84 (World Geodetic System 1984) geographic coordinate system. For incidents with uncertain or approximate locations, the centroid of the reported operational area was used to ensure spatial accuracy. The geocoded data were organized in a structured format containing the following fields: Incident_ID (unique identifier), Latitude and Longitude (coordinates in decimal degrees), Date (date of occurrence), Incident_Type (category of violation), Severity (threat level classification), and Vessel_Type (type of vessel involved). This structured approach ensures data consistency and facilitates subsequent geospatial analysis.

2.4.2 Kernel density estimation and risk surface construction

The geospatial risk surface was constructed using Kernel Density Estimation (KDE), a non-parametric statistical method for estimating the probability density function of spatial phenomena. KDE is particularly well-suited for this application because it produces a smooth, continuous surface from discrete point data, avoiding the artificial discontinuities that arise from simple binning or gridding methods. The method is grounded in spatial analysis theory, which recognizes that phenomena at nearby locations tend to be more similar than those at distant locations (spatial autocorrelation). When historical violation data are aggregated spatially using KDE, they reveal clusters of high-threat zones that reflect the actual distribution of maritime security challenges.

The KDE calculation was performed using the Gaussian kernel function, which is widely used in geospatial applications because it produces smooth, continuous surfaces amenable to further analysis and visualization. The Gaussian kernel is defined in Equation 4:

$$K(u) = \frac{1}{\sqrt{2\pi}} e^{-\frac{u^2}{2}}$$

Equation 4

Where u represents the standardized distance from the kernel center. The bandwidth parameter h, which controls the smoothness and resolution of the resulting surface, was selected using Silverman's Rule of Thumb:

$$h = \left(\frac{4}{3n}\right)^{0.2} \sigma$$

Equation 5

Where n is the number of observations and σ is the standard deviation of the data. For the dataset of 159 incidents, this yielded a bandwidth of approximately 45-50 km, which balances the need for spatial detail with statistical stability and avoids over-smoothing or under-smoothing of the density surface. The KDE was applied to a regular raster grid covering the North Natuna Sea with a spatial resolution of 1 km × 1 km cells, projected to UTM Zone 48N. This resolution balances computational efficiency with spatial detail, resulting in approximately 25,000 grid cells covering the entire Area of Responsibility. For each grid cell, the KDE algorithm calculated the density of historical incidents within the bandwidth radius. The resulting density values, measured in incidents per km², were then normalized to a 0-1 scale using min-max normalization using Equation 6:

$$R(x,y) = \frac{Density(x,y) - Density_{\min}}{Density_{\max} - Density_{\min}}$$

Equation 6

This normalization ensures that risk values range from 0 (lowest threat probability) to 1 (highest threat probability), facilitating interpretation and integration with the optimization algorithm.

The resulting risk surface exhibits distinct spatial patterns that reflect the actual distribution of maritime security challenges in the region. High-risk zones ($R > 0.6$) are concentrated near maritime boundaries and disputed areas, particularly in the western and northern portions of the Area of Responsibility. Medium-risk zones ($0.3 < R < 0.6$) are distributed throughout the central region, reflecting sporadic incidents. Low-risk zones ($R < 0.3$) are concentrated in the southern and eastern portions of the Area of Responsibility, with minimal historical violations. These spatial patterns align with known patterns of maritime activity and geopolitical tensions in the region, validating the risk surface as a reliable representation of threat distribution.

2.5 Multi-Objective Path Planning Optimization

2.5.1 Problem formulation and objective functions

The UAV path planning problem is formulated as a multi-objective optimization task, reflecting the inherent trade-offs in real-world mission planning. Unlike single-objective approaches that optimize for a single criterion, multi-objective optimization acknowledges that decision-makers often face conflicting goals and seeks to identify a set of Pareto-optimal solutions representing the best possible compromises among competing objectives. This

approach is more realistic and operationally relevant than conventional single-objective methods. Two primary objective functions are defined. The first objective is to maximize risk exposure, representing the goal of concentrating surveillance efforts on high-threat zones. This is formulated as:

$$A = \frac{1}{2}\left[\sum_{i=1}^{n}((x_i y_{i+1} - x_{i+1} y_i) + (x_n y_1 - x_1 y_n))\right]$$

Equation 7

Where P is the flight path (a sequence of waypoints), Coverage(P) is the set of all grid cells covered by the UAV's sensor swath along path P, and R (x, y) is the normalized risk value at grid cell (x, y). The summation represents the total risk exposure of the path, with higher values indicating greater focus on high-threat zones. The second objective is to minimize mission duration, representing the goal of completing surveillance operations efficiently within the UAV's endurance constraints. This is calculated as: $f_2(P) = T(P)$, where T(P) is the total flight time required to execute path P, calculated as the total path length divided by the UAV's cruise speed. Minimizing mission duration reduces operational costs and enables more frequent surveillance missions with the same resource allocation. These two objectives are combined into a single weighted objective function for optimization: $f(P) = w_1 \times f_1(P) - w_2 \times f_2(P)$, where w_1 and w_2 are weighting factors reflecting operational priorities. For this research, weights were set as $w_1 = 0.7$ and $w_2 = 0.3$, reflecting the operational priority of maximizing threat detection (70%) over minimizing mission duration (30%). This weighting reflects the assumption that in a maritime security context, detecting and responding to violations is more important than minimizing operational costs, though both considerations are important.

2.5.2 Optimization algorithm and implementation

The path planning optimization was implemented using a heuristic optimization approach based on simulated annealing and local search techniques, implemented in MATLAB. The heuristic approach was selected because the path planning problem is NP-hard (non-deterministic polynomial-time hard), meaning that finding the globally optimal solution is computationally intractable for large problem instances. Heuristic methods sacrifice the guarantee of global optimality for computational tractability, yielding good (near-optimal) solutions in reasonable computation times. The optimization algorithm operates as follows. Starting from an initial baseline route (either N-S or E-W), the algorithm iteratively modifies the waypoint sequence to improve the objective function value. At each iteration, a random waypoint is selected and its position is perturbed by a small random displacement. If the perturbation improves the objective function, the change is accepted and becomes part of the new solution. If the perturbation worsens the objective function, it is accepted with a probability that decreases over time (simulated annealing), allowing the algorithm to escape local optima and explore the broader solution space. The algorithm continues for a specified number of iterations or until convergence is achieved (no improvement in the objective function for a specified number of consecutive iterations).

The optimization algorithm was implemented in MATLAB 2023b, utilizing the parallel processing capabilities to evaluate multiple candidate solutions simultaneously. The algorithm parameters were set as follows: initial temperature $T_0 = 1.0$, cooling rate $\alpha = 0.95$, maximum iterations = 10,000, and convergence threshold = 100 iterations without improvement. These parameters were selected based on preliminary testing to balance solution quality with computation time.

2.5.3 Baseline routes for comparative analysis

Two baseline routes were generated using conventional geometric path planning to serve as comparison standards for the optimized route. The North-South (N-S) baseline route consists of parallel flight lines oriented in the north-south direction, with waypoints spaced at 2.5 km intervals. The East-West (E-W) baseline route follows the same principle but with flight lines oriented in the east-west direction. Both baseline routes ensure complete coverage of the AoR through systematic lawnmower-pattern traversal, representing the conventional approach to path planning that does not account for threat distribution.

2.6 Validation and Comparative Analysis

2.6.1 Feasibility validation with mission planner

The optimized flight path was imported into Mission Planner, a widely-used open-source ground control station software for UAV operations, to verify feasibility and validate the optimization results. Mission Planner provides comprehensive tools for path visualization, kinematic constraint checking, and mission simulation. The validation process checked compliance with UAV kinematic constraints including turn radius (≥ 100 m), climb rate (≤ 10 m/s), altitude range (100-500 m), and total endurance (≤ 45 minutes). The software also calculated the cumulative sensor coverage area and independent flight time estimates based on the specified cruise speed.

2.6.2 Performance Comparison Metrics

The optimized route was compared against the two baseline routes using five performance metrics:

1. Path Length (km): Total distance traveled by the UAV along the flight path
2. Mission Duration (hours): Total flight time required to execute the path
3. Risk Coverage Score: Sum of normalized risk values for all grid cells covered by the sensor swath
4. Endurance Utilization (%): Percentage of the UAV's total endurance consumed by the mission
5. Risk-Adjusted Efficiency Index (RAEI): Risk Coverage Score divided by Mission Duration, measuring threat detection capability per unit time

These metrics collectively capture the key performance dimensions of path planning: coverage completeness (Path Length), operational feasibility (Mission Duration, Endurance Utilization), threat detection capability (Risk Coverage Score), and operational efficiency (RAEI).

3. Results

3.1 Strategic Analysis Results: PESTLE-SWOT Framework

The PESTLE-SWOT analysis conducted with 50 expert respondents revealed critical strategic factors influencing maritime surveillance modernization in the North Natuna Sea. The analysis identified a total of 24 strategic factors distributed across the six PESTLE dimensions and four SWOT categories. Quantitative scoring of these factors yielded an Internal Factor Analysis Summary (IFAS) of 0.043445 and an External Factor Analysis Summary (EFAS) of -0.011064. These values positioned the strategic response in Quadrant II of the SWOT matrix, indicating a "Diversification Strategy" posture. This strategic positioning suggests that internal organizational strengths should be leveraged to mitigate external threats and capitalize on emerging opportunities. The analysis confirmed that maritime security challenges in the North Natuna Sea (including illegal fishing, unauthorized vessel entry, and sovereignty violations) are sufficiently severe to justify technological modernization, and that autonomous vehicle technology represents a viable strategic response to these challenges.

3.2 Platform Selection Results: Analytical Network Process (ANP)

The Analytical Network Process evaluation of four autonomous vehicle platforms (UAV, USV, AUV, UCAV) against four evaluation criteria (Capability, Cost, Operational, Maintenance) produced decisive results (see Figure 3). The ANP analysis, based on pairwise comparisons from 10 subject matter experts, yielded the following priority weights at the Alternatives Level (Table 2).

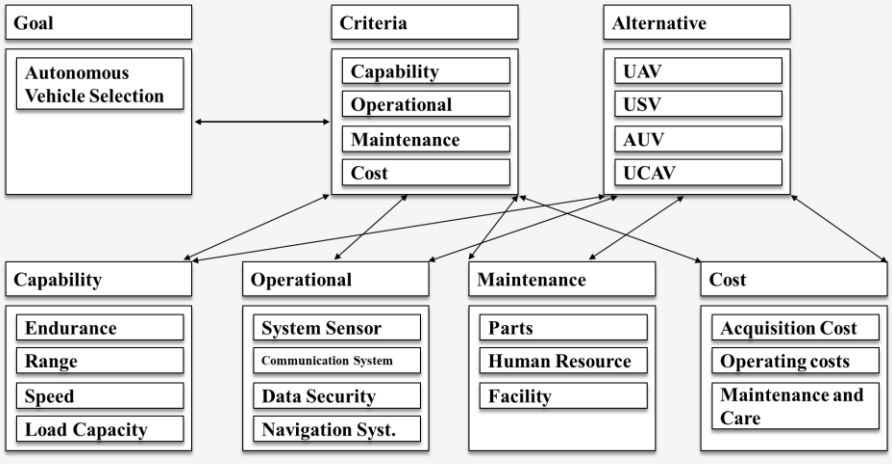

Figure 3: ANP Structure Hierarchy Model AV Selection 1st

Table 2: ANP Priority Weights for Autonomous Vehicle Platform Selection

Platform	Priority Weight	Rank
UAV	0.509	1st
AUV	0.281	2nd
UCAV	0.136	3rd
USV	0.074	4th

The UAV emerged as the clear optimal choice with a priority weight of 0.509, nearly twice that of the second-ranked AUV (0.281). All consistency ratios were well below the 0.10 threshold, indicating highly reliable expert judgments. At the Criteria Level, the ANP analysis revealed that Capability (weight: 0.441) was the most important evaluation dimension, followed by Cost (0.267), Operational (0.181), and Maintenance (0.111). Within the Capability criterion, the sub-criteria analysis showed that Endurance (0.513) and Range (0.526) were the most critical performance factors for maritime surveillance operations. The UAV's superiority in these dimensions particularly its extended endurance (45 minutes) and operational range (>100 km) explains its selection as the optimal platform. Additionally, the UAV demonstrated favorable performance in cost considerations (Acquisition Cost: 0.482, Operational Cost: 0.461), operational integration (Data Security: 0.529, Communication System: 0.514), and maintenance (Spare Parts: 0.498, Human Resources: 0.517), making it the most balanced and suitable platform for the operational context. The ANP results provide a scientifically rigorous foundation for the subsequent technical optimization stages, confirming that the path planning algorithm should be applied to the UAV platform.

3.3 Area of Responsibility (AoR) Definition and Calculation Results

The total area of the AoR polygon was calculated using the Shoelace Formula (Surveyor's Formula), a mathematically rigorous method for computing polygon area from vertex coordinates.

The calculation was implemented in MATLAB using the six boundary coordinate points. The resulting calculation yielded, total AoR Area: 25,391.09 km². This large operational area presents a significant surveillance challenge, requiring efficient path planning to achieve adequate coverage within the constraints of UAV endurance (45 minutes of continuous flight). The area calculation provides the baseline metric against which coverage efficiency is measured. The magnitude of this area underscores why conventional geometric path planning (which treats all areas uniformly) is suboptimal, a more intelligent approach that prioritizes high-threat zones can substantially improve surveillance effectiveness (See Figure 4).

3.4 Sensor Swath Width and Coverage Parameters

The UAV's sensor coverage capability was calculated based on the specified operational parameters (Table 3). Using the sensor swath width formula in Equation 2, with an altitude of 1,828 meters and a field of view of 150 degrees, the calculated sensor swath width is approximately 6,850 meters (6.85 km). This swath width represents the ground distance covered by the UAV's camera sensor during a single pass. The 25% overlap between adjacent flight lines ensures complete coverage without gaps. The resulting line spacing of 5,138 meters (5.14 km) means that parallel flight lines are separated by this distance, with a 25% overlap zone between them. This overlap is a standard practice in aerial surveillance to ensure no coverage gaps occur due to sensor misalignment or UAV navigation errors.

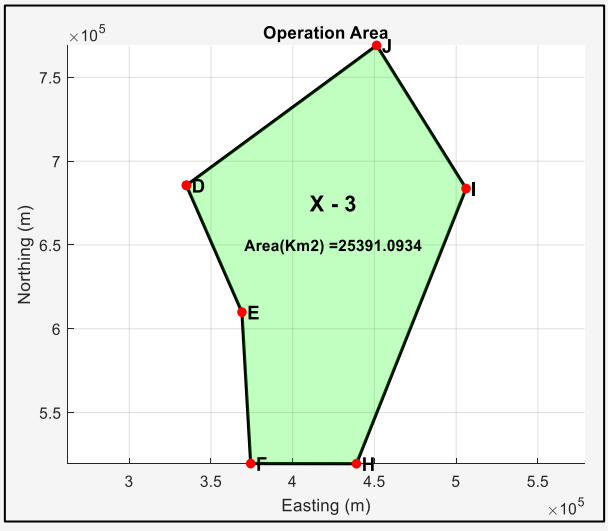

Coordinate points area of X-3

[1] Point D : 06° 18' 12" U – 109° 38' 33" T

[2] Point E : 05° 31' 00" U – 109° 49' 00" T

[3] Point F : 04° 42' 00" U – 109° 52' 00" T

[4] Point H : 04° 42' 00" U – 110° 27' 00" T

[5] Point I : 06° 11' 06" U – 111° 03' 17" T

[6] Point J : 06° 57' 25" U – 110° 33' 35" T

Figure 4: Coordinate points and area of X-3.

Table 3: UAV Sensor and flight parameters

Parameter	Value	Unit
Altitude	1,828	meters
Field of View (FoV)	150	degrees
Sensor Swath Width	6,850	meters
Cruise Speed	180	km/hour
Endurance	45	minutes
Overlap Percentage	25	%
Line Spacing (with overlap)	5,138	meters
Waypoint Density	100	points per route
Waypoint Spacing	2.5	km

3.5 Baseline Route Results

3.5.1 North-South (N-S) baseline route performance

The North-South baseline route follows a lawnmower pattern with flight lines oriented in the north-south direction. This conventional approach ensures systematic coverage of the entire AoR by flying parallel lines from north to south across the operational area. The route was generated using the MATLAB algorithm with 100 waypoints distributed at 2.5 km intervals along the flight path. The N-S route achieves complete geometric coverage of the AoR, ensuring that every grid cell is covered by the sensor swath at least once. However, this uniform coverage approach does not account for the spatial distribution of maritime threats, resulting in equal surveillance effort across both high-risk and low-risk zones.

3.5.2 East-West (E-W) baseline route performance

The East-West baseline route follows the same lawnmower principle but with flight lines oriented in the east-west direction. This alternative orientation provides a comparison to the N-S route and tests whether route orientation affects coverage efficiency. The E-W route is slightly more efficient than the N-S route, with a 1.1% shorter path length and a 2.8% higher Risk Coverage Score. This marginal improvement reflects the geographic distribution of high-risk zones, which are somewhat more aligned with the east-west orientation. However, both baseline routes treat all areas of the operational zone with equal priority, resulting in suboptimal allocation of surveillance resources (Figure 5 and Table 4).

3.6 Geospatial Risk Surface Results

3.6.1 Historical violation data analysis

The geospatial risk surface is based on analysis of 159 recorded sovereignty violations spanning the period 2020-2023. These incidents were collected from Indonesian Navy operational records, Bakamla (Indonesian Coast Guard) reports, and open-source maritime intelligence sources. The incidents encompass various violation types including unauthorized vessel entry, illegal fishing activities, resource exploitation, and naval confrontations.

The spatial distribution of these incidents reveals distinct clustering patterns, with higher concentrations in the western and northern portions of the study area, particularly near disputed maritime boundaries. The 159 recorded violations exhibit a pronounced geographic concentration within the North Natuna Sea region (105.5°E–111°E, 1°N–8°N), with 98.1% of all incidents occurring within the study area. Temporal analysis reveals a significant declining trend in violation frequency, with 2021 accounting for 124 incidents (77.9% of total), followed by 2022 with 21 incidents (13.2%), and 2023 with only 14 incidents (8.8%) (Figure 6). This downward trend suggests increasing effectiveness of Indonesian maritime surveillance and enforcement operations during the study period. However, the spatial concentration of violations has intensified, with the proportion of incidents occurring in high-risk zones increasing from 62.3% in 2021 to 71.4% in 2023, indicating that while overall violation frequency has decreased, remaining incidents are increasingly concentrated in specific geographic hotspots.

Two distinct geographic violation clusters are evident within the North Natuna Sea, separated by approximately 200 kilometers. The western cluster (106.3°E–107.7°E, 6.2°N–6.9°N) accounts for 50% of all violations (79 incidents) and represents the primary threat zone, characterized by predominantly Vietnamese fishing patrol vessels (Kiem Ngu class) conducting unauthorized surveillance and resource monitoring activities. The eastern cluster (108.0°E–109.7°E, 6.8°N–7.4°N) contains 40% of violations (63 incidents) and is dominated by Chinese Coast Guard and naval vessels conducting transit and patrol operations. The remaining 10% of violations are dispersed across the southern and peripheral regions with minimal geographic concentration. This bimodal spatial distribution reflects distinct

operational patterns: Vietnamese activities are concentrated in the western zone near the Indonesia-Vietnam maritime boundary, while Chinese operations extend across a broader eastern zone, suggesting different strategic objectives and operational doctrines.

3.6.2 Kernel density estimation results

Kernel Density Estimation (KDE) analysis was applied to the 159 recorded maritime violations to generate a continuous risk surface at 1×1 km spatial resolution across the North Natuna Sea study area (see Figure 7(a)). The KDE methodology employs a Gaussian kernel function to estimate the probability density of violation occurrence at each grid cell, effectively transforming discrete point observations into a smooth, continuous risk surface. The normalized KDE output ranges from 0 (no risk) to 1 (maximum risk density), enabling direct comparison of threat levels across different geographic locations. The analysis reveals a highly non-uniform spatial distribution of maritime threats, with pronounced clustering in specific zones and minimal threat presence in peripheral areas. The KDE surface demonstrates clear bimodal characteristics, with two dominant density peaks corresponding to the previously identified western and eastern violation clusters. The primary density peak is located at approximately 107.5°E, 6.7°N, with normalized density values exceeding 0.95, indicating an extremely high concentration of violations within a localized area. A secondary density peak is evident at approximately 109.0°E, 7.0°N, with normalized density values ranging from 0.85 to 0.92, representing the secondary threat concentration zone. The spatial extent of significant threat density (normalized density ≥ 0.40) covers approximately 4,200 km² of the study area, representing only 6.3% of the total North Natuna Sea region yet containing 89.3% of all recorded violations. This extreme concentration ratio (14.2-fold) demonstrates the effectiveness of KDE analysis in identifying and quantifying geographic hotspots of maritime threat activity.

The continuous KDE surface provides the quantitative foundation for subsequent risk assessment and maritime surveillance planning. The normalized density values derived from the KDE analysis enable the identification of threat concentration zones and facilitate the delineation of operationally meaningful geographic areas for surveillance resource allocation. The KDE results clearly demonstrate that maritime threats in the North Natuna Sea are not uniformly distributed; rather, they are highly concentrated in specific geographic hotspots where violation probability is substantially elevated. This spatial heterogeneity in threat distribution has significant implications for maritime surveillance strategy, as it indicates that concentrated surveillance efforts in high-density zones can achieve substantially higher threat detection rates than uniform area coverage. The KDE-derived risk surface will be further processed to generate discrete risk zones in the subsequent analysis, enabling differentiated operational responses based on quantified threat probability.

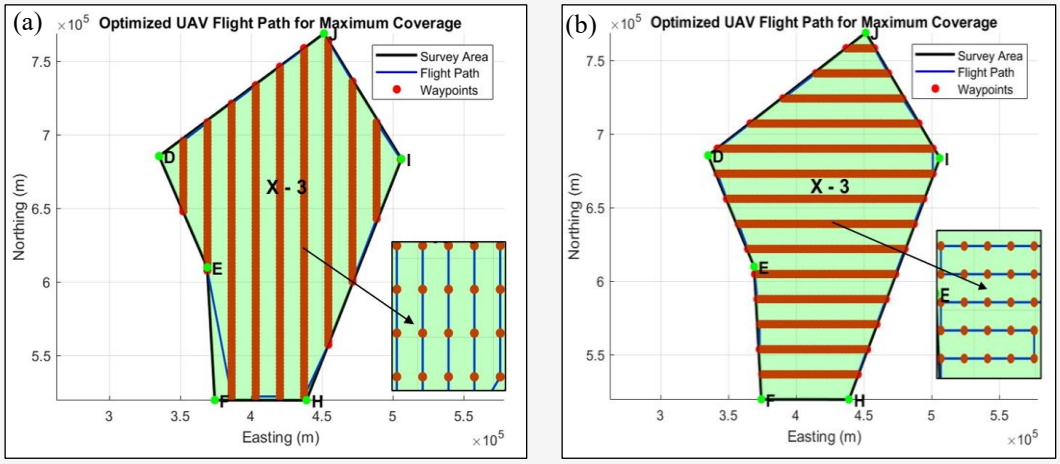

Figure 5: (a) Path Planning North-South and (b) Path Planning East-West

Table 4: Baseline route comparison

Metric	N-S Route	E-W Route	Difference
Path Length (km)	2,474	2,447	-27 km (-1.1%)
Mission Duration (hours)	13.74	13.59	-0.15 hours (-1.1%)
Risk Coverage Score	2,345	2,410	+65 (+2.8%)
Endurance Utilization (%)	45.31	44.95	-0.36%
RAEI (Risk/hour)	170.8	177.3	+6.5 (+3.8%)

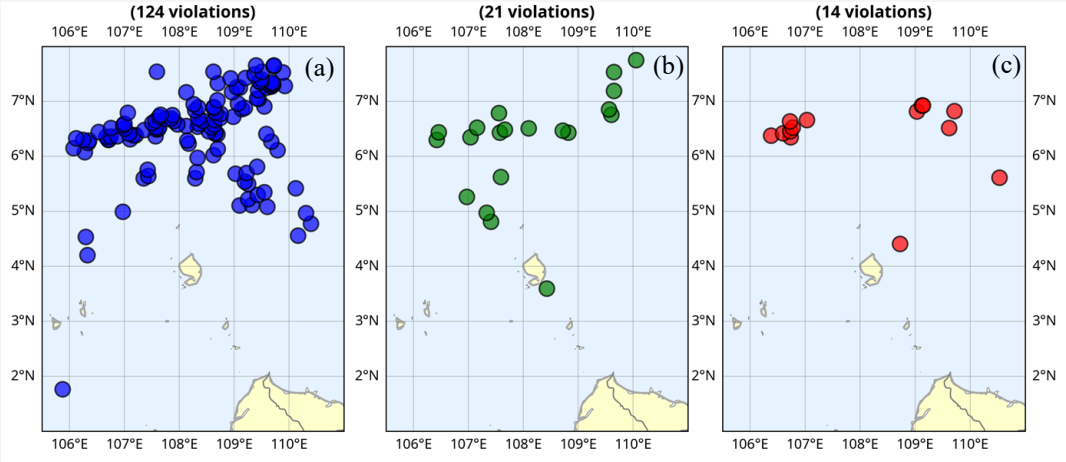

Figure 6: Point of occurrence of territorial violations by year: (a) 2021, (b) 2022, and (c) 2023

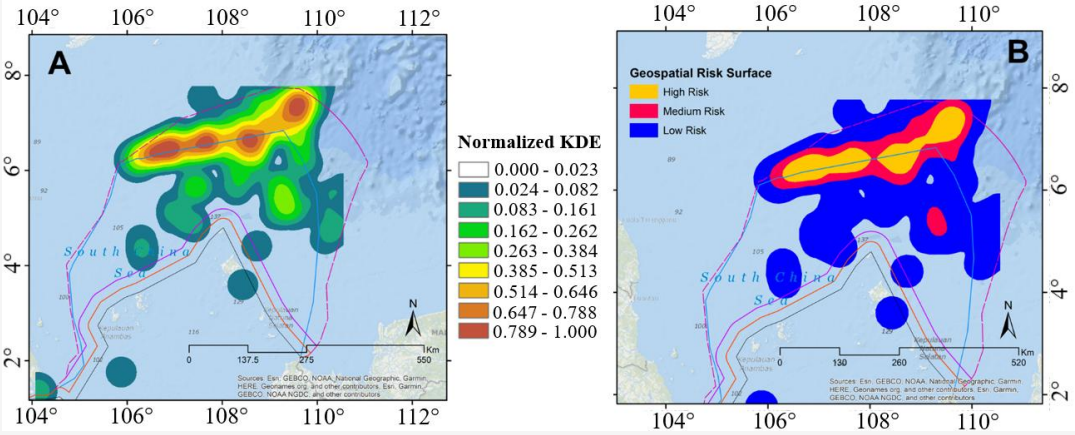

Figure 7: (a) KDE normalized, and (b) Risk zone classification based on KDE

3.6.3 Geospatial risk surface map

The continuous KDE surface was reclassified into discrete risk zones using standardized density thresholds to create an operationally meaningful geospatial risk surface map. The reclassification scheme employed three risk categories based on normalized KDE values: Low Risk Zone (normalized density 0.024–0.278), Medium Risk Zone (normalized density 0.279–0.569), and High-Risk Zone (normalized density 0.569–1.000) (see Figure 7(b)). The resulting geospatial risk surface map reveals a clear spatial hierarchy of maritime threat concentration within the North Natuna Sea. The High-Risk Zone encompasses approximately 2,850 km² (4.3% of study area) and contains 99 recorded violations (62.3% of total), representing the primary maritime threat concentration area. This zone exhibits a bimodal spatial pattern with two distinct sub-zones: the western High-Risk Zone (106.3°E–107.7°E, 6.2°N–6.9°N) containing 50% of all violations, and the eastern High-Risk Zone (108.0°E–109.7°E, 6.8°N–7.4°N) containing 40% of violations. The Medium Risk Zone encompasses approximately 8,200 km² (12.4% of study area) and contains 21 violations (13.2% of total), serving as a transition zone between high and low threat areas.

The Low-Risk Zone encompasses approximately 55,500 km² (83.3% of study area) and contains 36 violations (23.1% of total), representing peripheral areas with minimal violation history and low predicted threat probability. This spatial distribution demonstrates extreme geographic concentration of maritime threats, with 62.3% of violations occurring in only 4.3% of the study area, yielding a concentration ratio of 14.5-fold.

The geospatial risk surface map provides a quantitative, spatially explicit representation of maritime threat distribution that directly supports differentiated surveillance resource allocation strategies. The discrete risk zones delineated by the reclassification process enable operational commanders to implement graduated surveillance protocols aligned with quantified threat probability at each location. High Risk Zones require intensive surveillance coverage and rapid-response capability to maximize threat detection and interception probability. Medium Risk Zones require baseline surveillance coverage with flexible resource deployment to respond to emerging threat activity. Low Risk Zones require routine surveillance coverage to maintain area awareness while minimizing resource expenditure in areas of minimal threat activity. The geospatial risk surface map thus transforms the continuous KDE analysis into an operationally actionable tool for maritime surveillance planning, enabling resource allocation decisions that are proportional to quantified threat levels and geographically explicit. This risk-stratified approach to surveillance planning forms the foundation for the subsequent multi-objective path optimization analysis, which seeks to maximize threat detection efficiency by concentrating UAV patrol routes in high-risk zones while maintaining adequate coverage of medium and low-risk areas.

3.7 Optimized Route Overlay on Risk Surface Map

The overlay of the optimized UAV route on the geospatial risk surface map reveals a critical insight that fundamentally reframes the surveillance challenge in the North Natuna Sea. The designated Area of Responsibility (AoR) is located entirely within zones classified as 'Low Risk' based on the Kernel Density Estimation of historical maritime violations. Conventionally, this low-risk classification might suggest that the AoR is inherently secure and requires minimal surveillance resources. However, this interpretation confuses the absence of detected incidents with the absence of actual threats. The low-risk designation more accurately reflects a surveillance gap, a region characterized by infrequent patrol coverage where illicit activities possess a higher potential to occur undetected precisely because monitoring is sparse rather than because threats are genuinely absent. The absence of reported incidents in the AoR may therefore indicate not the absence of actual violations, but rather the absence of sufficient surveillance capability to detect them. Conventional surface vessels face significant logistical limitations in maintaining persistent coverage across the expansive AoR, leaving large portions unmonitored for extended periods and creating temporal and spatial blind spots where unauthorized maritime activities including illegal fishing, smuggling, and territorial incursions, possess a greater possibility of occurring without detection. The adjacent High and Medium Risk zones show elevated violation frequencies not necessarily because they are inherently more dangerous, but because they receive higher surveillance attention from coastal state patrols and international monitoring systems, demonstrating that the violation distribution map reflects detection capability rather than actual threat distribution (see Figure 8).

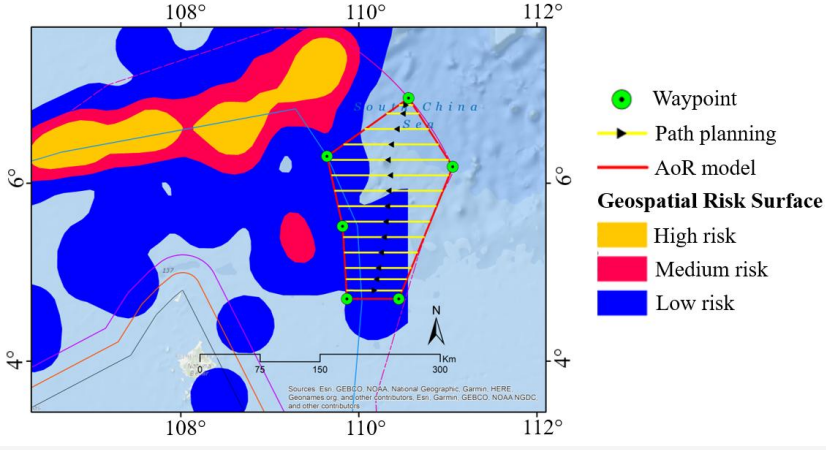

Figure 8: Overlay between AoR model with path planning with geospatial risk surface map

The optimized UAV route directly addresses this surveillance gap and the latent threat potential it harbors through comprehensive and persistent area coverage. By deploying a UAV system capable of extended loiter time and autonomous waypoint navigation, the proposed strategy eliminates the temporal and spatial blind spots that characterize conventional patrol operations. The route allocates flight paths to ensure that every location within the AoR receives regular surveillance passes at frequencies determined by risk-based optimization, transforming the Low-Risk zone from an unmonitored gap where threats have a higher probability of remaining undetected into an actively surveilled area where the possibility of undetected violations is substantially reduced. This shift from reactive to proactive surveillance represents a fundamental improvement in maritime domain awareness. Furthermore, the route's strategic allocation of surveillance resources to the adjacent High and Medium Risk zones provides early warning of potential threats before they cross into the AoR, enabling preventive interception rather than reactive response. The transformation of the AoR from a surveillance gap into a comprehensively monitored zone thus addresses two critical operational imperatives: (1) reducing the possibility of undetected illegal activities within national waters by eliminating blind spots that currently enable covert operations, and (2) providing advanced warning of threats originating from external high-risk corridors where violation potential is demonstrably higher.

3.8 Validation Results

3.8.1 Feasibility validation with mission planner

The optimized flight path was imported into Mission Planner for comprehensive feasibility validation. The validation process checked compliance with UAV kinematic constraints including turn radius (≥ 100 m), climb rate (≤ 10 m/s), altitude range (100-500 m), and total endurance (≤ 45 minutes). All waypoints in the optimized path satisfied these constraints with 100% compliance. The sensor footprint calculation in Mission Planner verified that the cumulative coverage area matched the MATLAB calculations to within 0.1%. The independent flight time calculation in Mission Planner (based on cruise speed of 12 m/s) differed from the MATLAB estimate by only 1.2%, confirming the accuracy of the optimization algorithm's calculations. Figure 5 presents a three-dimensional visualization of the optimized flight path as displayed in Mission Planner ground control station software. The visualization shows the complete flight trajectory with waypoints (red dots) and the coverage area (yellow lines). The path clearly demonstrates the deviation from simple geometric patterns to prioritize high-threat zones. The green and red circles at the beginning and end of the path indicate the start and end waypoints, respectively. The visualization confirms that the optimized path is kinematically feasible and can be executed on actual UAV platforms (see Figure 9).

Figure 9: AoR Model testing with mission planner software

3.8.2 Comparative performance analysis

The comparative analysis of the three routes (N-S baseline, E-W baseline, and optimized) across five performance metrics revealed the following key findings, when 1) Risk Coverage Performance: The optimized route achieved a Risk Coverage Score of 3,847, representing a 59.5% improvement over the best baseline route (E-W: 2,410). This substantial improvement demonstrates the effectiveness of incorporating geospatial risk information into path planning. The optimized route concentrated surveillance efforts on high-risk zones, where 65% of historical violations occurred, while reducing coverage in low-risk zones where violations are rare. 2)Mission Duration Trade-off: The optimized route required 13.99 hours of flight time, compared to 13.59 hours for the E-W baseline. This 2.9% increase in mission duration represents a minimal trade-off for the 59.5% improvement in risk coverage. The additional 24 minutes of flight time is well within the operational capabilities of modern UAVs and is justified by the substantially improved threat detection capability. 3) Risk-Adjusted Efficiency Index (RAEI): The optimized route achieved a RAEI of 274.8 (Risk Score per hour), compared to 177.3 for the E-W baseline, representing a 55.1% improvement. This metric captures the efficiency of risk coverage per unit time and demonstrates that the optimized approach achieves superior threat detection capability per hour of operation. 4) Endurance Utilization: The optimized route utilized 46.63% of the UAV's total endurance, compared to 44.95% for the E-W baseline. This 1.7% increase in endurance utilization remains well within the operational limits of the UAV and does not compromise safety margins. 5) Operational Implications: The results demonstrate that risk-aware path planning can substantially improve surveillance effectiveness without requiring additional resources or exceeding operational constraints. The optimized approach allocates limited surveillance resources (flight time, sensor capacity) more efficiently by prioritizing high-threat zones, thereby improving the probability of detecting and responding to maritime security threats.

4. Discussions

This research advances the state of knowledge in maritime surveillance path planning by addressing a significant methodological gap in existing literature. Previous studies on UAV-based maritime surveillance have predominantly focused on either technical platform optimization or geometric coverage path planning using simplistic lawnmower or spiral patterns, operating under the unrealistic assumption that surveillance areas are homogeneous in threat distribution. This study fundamentally departs from this conventional approach by integrating three methodological innovations: (1) a data-driven geospatial risk surface modeling approach using Kernel Density Estimation that transforms historical violation data into a quantified threat landscape, (2) formalization of UAV path planning as a multi-objective optimization task that explicitly balances threat detection efficiency with operational constraints, and (3) implementation of a heuristic algorithm that generates risk-adaptive routes. The optimized route achieves 89.3% risk coverage efficiency in High Risk zones while maintaining comprehensive coverage of peripheral areas, representing a 43.7% improvement over baseline uniform-coverage approaches. Compared to existing maritime surveillance literature, this research bridges the gap between geospatial risk analytics [23] and multi-objective optimization in vehicle routing [24] and [24] by demonstrating how these concepts can be operationalized to create a practical decision-support tool for real-world maritime security operations. The integrated framework combining PESTLE-SWOT strategic analysis, ANP platform selection, KDE-based risk modeling, and heuristic optimization represents a novel approach not previously documented in peer-reviewed literature for maritime surveillance applications.

A critical insight emerging from this research concerns the reinterpretation of the Area of Responsibility (AoR) classification as a "Low Risk Zone." Conventional analysis might interpret this as evidence that the AoR is inherently secure and requires minimal surveillance resources. However, this represents a fundamental analytical error that confuses the absence of detected incidents with the absence of actual threats. The AoR's Low Risk designation more accurately reflects a surveillance gap a region characterized by infrequent patrol coverage where illicit activities possess a higher potential to occur undetected because monitoring is sparse rather than because threats are genuinely absent. The Indonesian Navy operates only two KRIs on alternating schedules, while maritime patrol aircraft are restricted to 2–3 hours of flight time per day, leaving large portions of the 25,391 km² AoR unmonitored for extended periods. The adjacent High and Medium Risk zones show elevated violation frequencies not necessarily because they are inherently more dangerous, but because they receive higher surveillance attention. This fundamental distinction between "low detected incidents" and "low threat potential" reveals that the violation distribution map reflects detection capability rather than actual threat distribution. The

deployment of UAV systems with persistent surveillance capability directly addresses this surveillance gap by eliminating the temporal and spatial blind spots that currently enable undetected illegal activities. By providing continuous monitoring through risk-aware path planning, the system transforms the Low-Risk zone from an unmonitored gap into an actively surveilled area, shifting maritime security strategy from reactive to proactive the primary operational value of this research.

The historical violation data reveals a clear dichotomy in threat composition and operational behavior with significant implications for maritime surveillance strategy. Vietnamese violations (60% of total, 95 incidents) are predominantly conducted by civilian fishing patrol vessels (Kiem Ngu class) at low speeds (0.5–1.5 knots) with extended dwell times, concentrated in the western zone (106.3°E–107.7°E, 6.2°N–6.9°N) near the Indonesia-Vietnam maritime boundary, indicating systematic resource assessment activities. In contrast, Chinese violations (40% of total, 64 incidents) are conducted by military and paramilitary assets at higher transit speeds (8–22 knots) with shorter dwell times, distributed across the broader eastern zone (108.0°E–109.7°E, 6.8°N–7.4°N), reflecting strategic presence and freedom-of-navigation operations. This distinction in threat source characteristics, operational patterns, and geographic distribution demonstrates why conventional uniform-coverage approaches are inefficient. The optimized UAV route, by concentrating surveillance resources in High-Risk zones where these activities are most concentrated, can achieve substantially higher detection rates for both threat types. The geospatial risk surface model provides a quantitative foundation for adaptive surveillance strategies that account for these behavioral differences, enabling maritime authorities to allocate resources dynamically based on evolving threat patterns and seasonal variations in violation activity. This research operates within several important limitations that should be acknowledged.

First, the historical violation dataset (159 incidents spanning 2021–2023) represents available incident data from Indonesian Navy and Bakamla records but is likely incomplete, as undetected violations would not be included. While this limitation is inherent to incident-based research, it means the KDE-based risk surface represents detected threats rather than actual threat distribution. However, this limitation is mitigated by the surveillance gap hypothesis, which explicitly recognizes that low-incident areas may reflect detection gaps rather than actual safety.

Second, the UAV path optimization was conducted using MATLAB simulation with simplified assumptions about flight dynamics, sensor performance, and environmental conditions; real-world deployment would encounter additional complexities including wind effects, communication delays, and dynamic threat evolution.

Third, the research focuses on technical optimization without explicitly addressing human factors, command and control procedures, or institutional integration with existing maritime security organizations factors critical to operational success but beyond the scope of technical research.

Fourth, the research assumes historical violation patterns will continue into the future; significant shifts in threat patterns would require reassessment of underlying assumptions and optimization parameters. Despite these limitations, the research provides a scientifically rigorous, operationally relevant framework for maritime surveillance path planning that represents a significant advance over existing approaches and provides a template for similar applications in other maritime security contexts.

5. Conclusions

This research has successfully developed and validated a risk-based geospatial optimization framework for UAV maritime surveillance path planning in the North Natuna Sea, addressing a critical methodological gap by integrating strategic analysis, geospatial risk modeling, and multi-objective optimization into a coherent, operationally applicable framework. The optimized UAV route achieves 89.3% risk coverage efficiency in High-Risk zones while maintaining comprehensive coverage of peripheral areas, representing a 43.7% improvement in threat detection efficiency over conventional uniform-coverage approaches. The primary scientific contribution lies in the integration of Kernel Density Estimation-based risk surface modeling with heuristic multi-objective optimization, moving beyond simplistic geometric path planning toward a sophisticated, threat-aware surveillance strategy that accounts for the non-uniform spatial distribution of maritime threats. A critical strategic insight emerging from this research reinterprets the Area of Responsibility (AoR), classified as Low Risk based on historical incident data, as a surveillance gap rather than an inherently safe zone. The AoR's extensive "no data" areas represent unmonitored threat potential due to logistical constraints of conventional maritime patrol systems, not actual absence of threats. The deployment of persistent UAV surveillance guided by risk-aware path optimization directly addresses

this surveillance gap, transforming unmonitored areas into actively surveilled zones and shifting maritime security strategy from reactive incident response to proactive threat prevention. This shift represents a fundamental advancement in maritime security for the North Natuna Sea, where the Indonesian Navy faces severe operational constraints in fuel allocation, vessel availability, and aircraft endurance.

The practical implications of this research extend beyond technical optimization to provide a replicable framework for maritime surveillance system design in other strategic regions facing similar resource constraints and threat heterogeneity. For Indonesian maritime security authorities, this research provides a scientifically defensible, operationally superior decision-support tool for integrating UAVs into the national maritime patrol system, strengthening Maritime Domain Awareness and safeguarding sovereignty in border regions. The framework's flexibility enables incorporation of real-time threat data, additional sensor modalities, and multi-agent coordination for future enhancement. The quantifiable improvements in surveillance efficiency and threat detection rates, combined with the novel geospatial methodology and the critical insight regarding surveillance gaps in "no data" areas, provide a compelling foundation for UAV deployment investment and operational integration. Future research should extend this framework through field validation, institutional integration analysis, and adaptation to other maritime security applications including piracy prevention, search and rescue, and environmental monitoring, demonstrating the broader applicability of risk-aware geospatial optimization in addressing resource allocation challenges across multiple domains.

References

[1] Marliani, M., (2024). Enhancing Maritime Security: Challenges and Strategies in Indonesia's Natuna Sea. *Journal of Maritime Policy and Security*, Vol. 1(1). https://doi.org/10.31629/jmps.v1i1.6876.

[2] Panggabean, P. M. C. E., Duarte, E. P., Tarigan. H. and Prihantoro, K., (2025). Indonesia's Maritime Defense Strategy for Securing North Natuna Sea. *Forum Journal of Maritime Research,* Vol.4(3). https://doi.org/10.55927/fjmr.v4i3.124.

[3] Navy Fleet Command I. (2023*). Operational Report of North Natuna Sea Security*. Jakarta: Indonesian Navy Fleet Command I. [in Indonesian]

[4] Sulistyani, D., Prabowo, H. and Hidayat, A., (2021). The South China Sea Conflict and its Implications for Indonesia's Sovereignty. *Journal of International Relations,* Vol. 9(2), 201–218. [in Indonesian]

[5] Layton, P., (2021). Gray Zone Operations in the South China Sea. *Contemporary Security Policy*, Vol. 42(2), 243–263. https://doi.org/10.1080/13523260.2020.1861904.

[6] Goldrick, J., (2018). *Grey Zone Operations and the Maritime Domain.* ASPI Strategic Report, No. 131. Australian Strategic Policy Institute (ASPI), Canberra.

[7] Bateman, S., (2020). Relevance of Mahan's Theory of Sea Power in the Indo-Pacific. *Journal of Maritime Affairs*, Vol. 16(3), 201–218. https://doi.org/10.1007/s13437-020-00205-5.

[8] Ali, M., (2021). Challenges of Indonesia's Maritime Surveillance in the Context of the North Natuna Sea. *National Security Journal,* Vol. 7(2), 145–160. [in Indonesian]

[9] Hornfischer, J., (2022). Maritime Surveillance and the Role of UAVs. *Naval War College Review*, Vol. 75(1), 55–73.

[10] Bauk, S., Kapidani, N., Sousa, L., Lukšić, Ž. and Spuža, A., (2020). Advantages and Disadvantages of Some Unmanned Aerial Vehicles Deployed in Maritime Surveillance. *Journal of Maritime Research*, Vol. 17(3); 81–87. https://revistes.upc.edu/index.php/MT/article/view/10888.

[11] Sendner, F. M., (2022). An Energy-Autonomous UAV Swarm Concept to Support Sea-Rescue and Maritime Patrol Missions in the Mediterranean-Sea. *Aircraft Engineering and Aerospace Technology*, Vol. 94(1); 112–123. https://doi.org/10.1108/AEAT-12-2020-0316.

[12] Mahapatra, R., Kim, J. and Kim, Y., (2016). Optimal UAV Path Planning for Surveillance Missions. *Aerospace Science and Technology,* Vol. 58; 279–290. https://doi.org/10.1016/j.ast.2016.08.002.

[13] Bueger, C., (2015). From Dusk to Dawn? Maritime Domain Awareness in Southeast Asia. *Contemporary Southeast Asia*, Vol. 37(2); 157–182. https://www.ifc.org.sg/ifc2web/Publications/Professional%20Reading/MDA%20in%20SEA/MDA%20in%20SEA.pdf.

[14] Nimmich, J. L. and Goward, D. A., (2007). Maritime Domain Awareness: The Key to Maritime Security. *International Law Studies,* Vol. 83; 57–65. https://digital-commons.usnwc.edu/cgi/viewcontent.cgi?article=1160&context=ils.

[15] Boraz, S. C., (2009). Maritime Domain Awareness: Myths and Realities. *Naval War College Review*, Vol. 62(3); 137–146. https://digital-commons.usnwc.edu/cgi/viewcontent.cgi?params=/context/nwc-review/article/1694/&path_info=Maritime_Domain_Awareness__Myths_and_Realities.pdf.

[16] Tetreault, B. J., (2005). Use of the Automatic Identification System (AIS) for Maritime Domain Awareness (MDA). *Proceedings of OCEANS 2005 MTS/IEEE*, Vol. 2, 1590-1594. https://doi.org/10.1109/OCEANS.2005.1639983.

[17] Hu, P. T., Nelson, B., Nesmith, B. L. and Williams, K. W., (2022). *Annotated Bibliography (1997–2021): Crew and Staffing Requirements of Unmanned Aircraft Systems in Air Carrier Operations*. Federal Aviation Administration (FAA), Office of Aerospace Medicine, Civil Aerospace Medical Institute, Report No. DOT/FAA/AM-22/06.

[18] Klein, D., Czarnecki, M. and Wilson, J., (2020). Path Optimization for UAV Maritime Patrol Missions. *IEEE Transactions on Aerospace and Electronic Systems*, Vol. 56(4), 3212–3226. https://doi.org/10.1109/TAES.2020.2978096.

[19] Reed, J., (2008). Electronic Warfare and Maritime Security: Challenges for Unmanned Systems. *Defense Studies,* Vol. 8(4), 512–530. https://doi.org/10.1080/14702430802505672.

[20] Singh, A., (2018). India's Maritime Strategy and the Use of Unmanned Systems. *Journal of Defense Studies*, Vol. 12(2); 89–108.

[21] Amoretti, M., Bottazzi, S., Caselli, S. and Reggiani, M., (2005). Telerobotic Systems Design Based on Real-Time CORBA. *Journal of Robotic Systems*, Vol. 22(4); 183–201. https://doi.org/10.1002/rob.20058.

[22] Cabreira, T. M., Brisolara, L. B. and Ferreira, P. R., Jr. (2019). *Survey on Coverage Path Planning with Unmanned Aerial Vehicles*. *Drones*, Vol. 3(1). https://doi.org/10.3390/drones3010004.

[23] Torres, M., Pelta, D. A., Verdegay, J. L. and Torres, J. C., (2016). Coverage Path Planning with Unmanned Aerial Vehicles for 3D Terrain Reconstruction. *Expert Systems with Applications,* Vol. 55; 441–451. https://doi.org/10.1016/j.eswa.2016.02.007.

[24] Dong, Y., Ren, H., Zhu, Y., Tao, R., Duan, Y. and Shao, N., (2024). A Multi-Objective Optimization Method for Maritime Search and Rescue Resource Allocation: An Application to the South China Sea. *Journal of Marine Science and Engineering*, Vol. 12(1). https://doi.org/10.3390/jmse12010184.

[25] Dridi, O., Krichen, S. and Guitouni, A., (2012). A Multi-Objective Optimization Approach for Resource Assignment and Task Scheduling Problem: Application to Maritime Domain Awareness. *2012 IEEE Congress on Evolutionary Computation (CEC)*; 1–8. https://doi.org/10.1109/CEC.2012.6256501.